

Mathematical algorithms for determination of mixed layer height from laser radar signals

Y. Bhavani Kumar¹ and S.Purusotham²

1. Project leader, LIDAR project, National Atmospheric Research Laboratory (NARL), Gadanki-517112, India

2. Research Scholar, Department of Mathematics, S.V.University, Tirupati – 517502, India

Abstract— This paper describes different mathematical algorithms used in the determination of mixed layer height (MLH) from the laser radar (lidar) signals. These methods are successfully applied to the indigenously developed portable lidar signals for retrieval of the depth of pollutants mixing in the lower atmosphere. The study also includes intercomparison between the methods.

Keywords- Portable lidar, Laser radar, lidar signal, ABL height, Analytical methods

I. INTRODUCTION

The Atmospheric boundary layer (ABL) is the lowest layer (1–3 km) of the atmosphere that is directly affected by interactions at the Earth's surface. Reference [1] defined the boundary layer as the lowest part of the atmosphere that is directly influenced by the presence of the Earth's surface, and responds to surface forcings with a timescale of about an hour or less. The ABL height plays a crucial role in the transport and diffusion of pollutants in the lower atmosphere. The ABL thickness is quite variable in space and time, ranging from hundreds of meters to a few thousand meters. It is practice in air pollution meteorology to use the term mixed layer (ML) since pollutants that are emitted into the ABL become gradually dispersed and mixed through the action of turbulence. The mixed layer depth (MLD) is the height of the top of the ML and is an important parameter to characterize the ABL and its structure. Measurements, parameterizations and predictions of the MLD have many theoretical and practical applications such as the prediction of pollutant concentrations, in numerical weather prediction and climate modeling [2,3] and the study of turbulence in ABL.

The optical power measured by laser radar is proportional to the particle content (aerosol content) of the atmosphere within boundary layer (BL). The lidar signal shows a strong backscattering within the BL, which decreases through a transition zone and becomes weak in the free troposphere (FT). By using aerosols as the tracers of atmospheric dynamics, laser radar can identify several dynamical parameters of the atmospheric boundary layer (ABL) such as boundary layer top and entrainment zone depth [4-9] in real-time with high temporal and spatial resolutions.

II. PORTABLE LASER RADAR

A portable laser radar system was successfully developed and made operational at the National Atmospheric Research Laboratory (NARL), an autonomous research institution under Department of Space, in 2004 for monitoring the boundary layer aerosol particles as the tracers of atmospheric dynamics [10]. The lidar system was developed under a project titled boundary layer lidar (BLL). The location of lidar site is Gadanki (13.5°N, 79.2°E; 375 m above *mean sea level*) situated close to *Tirupati*, a famous temple town, in the southern part of India.



Fig.1 The portable laser radar system at NARL site

The portable laser radar employs a diode-pumped Nd-YAG laser system, a co-axial transceiver for transmitting the laser pulses and detecting the collected photons, a dedicated data acquisition system, and a computer control and interface system (See Fig. 1). Pulses of light energy are transmitted from the telescope into the atmosphere. As the pulse propagates, part of it is scattered by molecules, water droplets, ice crystals, dust and haze aerosol in the atmosphere. A small portion of the light that scattered back is collected by the telescope and then detected. The distance to the particle layers

is inferred based on the time delay between each outgoing transmitted pulse and the backscattered signal. The detected signal is stored in bins according to how long it has been since the pulse was transmitted, which is directly related to how far away the backscatter occurred. The collection of bins for each pulse is called a profile. These lidars are smaller in size, reliable, and simple, coupled with its autonomous, eye-safe operation, save research money through simpler setup and reduced personnel needs, while producing higher quality data.

III. DETERMINATION OF ABL HEIGHT

The use of the laser radar technique for ranging the BL depends on the altitude resolved measurement of atmospheric backscatter intensity from outgoing laser radiation. The functional expression [11] that relates outgoing laser energy (E_0) and the backscattered signal $P(z)$ is given as

$$P(z) = KE_0O(z)\frac{\beta_T(z)}{z^2}T^2(z) + P_b \quad \text{--- (1)}$$

where E_0 laser pulse energy, K represents lidar system constant, $O(z)$ represents the overlap function (for portable lidar system, $O(z)=1$ for heights above 200 m AGL). Here AGL stands for above ground level. In the atmosphere, two types of optical scattering takes place, scattering by the *air molecules* and *solid particles* or *liquid droplets* suspended in the air. The received laser radiation measured by lidar is proportional to the effective backscattering from particles and molecules present in the atmosphere. The term $T(z)$ refers to the transmittance offered by the atmospheric path to the laser photons traveling from the ground to a given distance z .

The term P_b relates to the sky background contributed as noise to the signal counts. It is the number of photons detected from the background including any light sources other than the emitted laser light such as airglow emission, star light, and photodetector dark counts. The dark count is caused by spontaneous emission of photoelectrons from the cathode in the PMT. It may be mentioned here that the return signals, from ranges much above the signal range, where the count level was stable and constant over the integration period are considered as background. In this work, the background is determined by utilizing the signal returns in heights above 30 km. The lidar signal is need to be background corrected and transformed into a variable that removes the range square dependence, $X(z)$ [12] or its logarithm, $S(z)$ [13].

$$X(z) = [P(z) - P_b]z^2 \quad \text{--- (2)}$$

$$S(z) = \ln[X(z)] \quad \text{--- (3)}$$

A. Threshold method

The boundary layer (BL) height from lidar profiles is defined differently by numerous researchers. Reference [14] identified the BL height as the height where the signal backscatter begins to decrease from a relatively higher value to lower region. References [14] and [15] used simple signal threshold values. A number of threshold methods have been

proposed to determine the BL height from lidar signal profiles. One such method that involves a direct comparison of lidar backscatter signal, $P(z)$, with a fitted Rayleigh molecular backscatter profile is shown in Fig.2. The boundary layer height can be defined as the first altitude point for which the measured backscatter profile exceeds the Rayleigh model profile by some fixed amount, ϕ . Following reference [15], ϕ is chosen to be 25%, although it is noted that the boundary layer height retrieved by this method is not particularly sensitive to reasonable values of ϕ . Reference [16] has also employed this method to estimate the BL height from the lidar backscatter. However, in practice, threshold methods will often misidentify particulate layers above or below BL as the top of the BL and are thus not recommended [17].

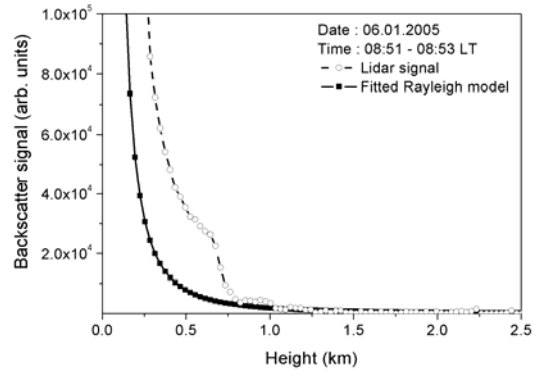


Fig.2 A lidar backscatter profile recorded at 08:51 LT on 06 January 2005. The Rayleigh model is fitted between the indicated altitudes.

B. Derivative methods

In this method of BL determination, the derivative of the signal will exhibit a strong negative peak. The BL height can be identified by the absolute minimum. Under derivative methods, gradient (GM), double gradient (DGM) and logarithmic gradient (LGM) are generally employed to determine the BL height from the lidar profiles.

1) Gradient Method

The lidar signal exhibits a strong backscattering within the BL, which decreases through a transition zone and becomes weak in the free troposphere (FT). This is explicitly clear for range corrected signal, $X(z)$, shown as a typical example in Fig.3(a). The data presented is obtained from the lidar system on 11 January 2005 at 22:00 LT. One can see an abrupt drop in backscatter intensity at the top of the BL, which can be considered as a gradient in the range corrected signal that appears to be a good option for determination of BL height. The GM method looks for the altitude (h_{GM}) of the absolute negative minimum of the first derivative of the $X(z)$

$$h_{GM} = \min\left\{\frac{d[X(z)]}{dz}\right\} \quad \text{--- (4)}$$

The application of gradient method to the lidar data is shown in Fig. 3(b). The estimated height h_{GM} is obtained as 800m in this case. In late seventies, reference [18] described BL height as the height at which a maximum negative gradient of laser backscatter in vertical direction occurs. Reference [14]

identified the BL height as the height where the signal backscatter begins to decrease from a relatively higher value to lower region. Reference [19] also mentioned the BL height as a zone of minimum in the vertical gradient of the backscatter as defined by [18]. A number of researchers have calculated the gradient of the signal with height and used the change in gradient as an indicator of the BL height [20, 21]. However, some times complex profiles show several minima exist over an extended height range and the absolute minimum does not always give the BL height. As the range corrected signal $X(z)$ is noisy, at heights near BL top, derivative of the $X(z)$ can present several small negative peaks and there will be a difficulty to determine the lowest negative peak. The effect of presence of several negative peaks has been discussed by [1].

2) Double gradient method (DGM)

Another mathematically similar method uses the minimum of the second order derivative of the range corrected signal, which is location of the inflection point, as the height. This method is known as the inflection point (IPM) or double gradient method (DGM).

$$h_{DGM} = \min \left\{ \frac{d^2[X(z)]}{dz^2} \right\} \quad \text{--- (5)}$$

Reference [22] used the absolute minimum of the second derivative that corresponds to the minimum of the second derivative of the range corrected signal $X(z)$ located just below h_{GM} . Limitations of IPM are found in the presence of elevated humid aerosol-laden layers whenever the inversion capping the mixed layer is weak [22]. Fig.3(c) shows the application of method to the lidar signal $X(z)$. The estimated height h_{DGM} is obtained as 750m in this case.

3) Logarithmic gradient method (LGM)

A variant method that uses the location of the maximum value of the logarithmic derivative of the range corrected signal is employed by [23] as the criteria for the BL height determination. The derivative of the logarithm of $S(z)$ is proportional to the aerosol extinction gradient and therefore it can also be used to detect the largest negative gradient. The logarithm gradient method (LGM) consists in finding the altitude, h_{LGM} , at which the minimum of the first derivative of the logarithm of $S(z)$ is reached [24].

$$h_{LGM} = \min \left\{ \frac{d[S(z)]}{dz} \right\} \quad \text{-- (6)}$$

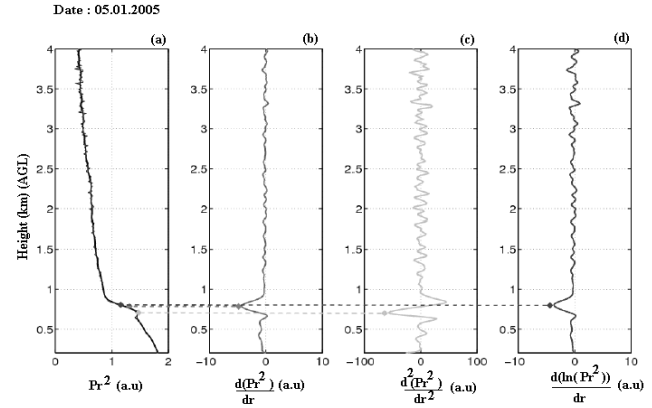


Fig.3 Application of derivative methods for determination of BL height (a) range corrected lidar signal (b) gradient method (c) double gradient method and (d) logarithmic gradient

Fig.3 (d) shows the use LGM to the lidar data. The calculated h_{LGM} height in this case study is 800 m. In general, inflection point or maximum derivative methods have the advantage of being independent of any arbitrary threshold values and show good accuracy when turbulent fluctuations are present [22]. However, as a practical matter, running derivatives are difficult to calculate in the presence of noisy data, particularly at longer ranges. Thus some type of spatial/or temporal averaging is required [17].

C. Variance method

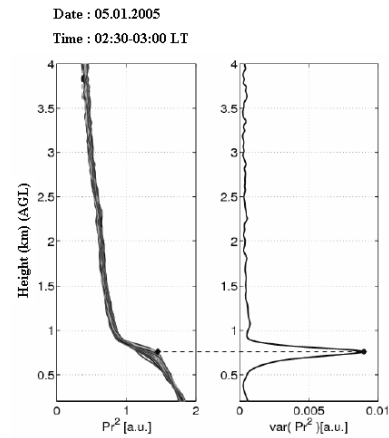


Fig.4. Plot showing several lidar range corrected signal profiles and the corresponding variance method output

The backscatter signal, in the BL, is the culmination of scattering from aerosols and molecules within the BL. At any given height, there is much greater variability in the aerosol distribution in the BL. Therefore, it is possible to use variance, σ^2 , of the backscattered signal to measure the BL height [25,26]. This method is also called the variance centroid method (VCM). In this method, the standard deviation is calculated from the temporal fluctuations of the range squared signal $X(z)$ at each altitude, as follows

$$\sigma_{X(z)} = \left(\frac{1}{N} \sum_{i=1, N} \left[X_i(z) - \bar{X} \right]^2 \right) \quad \text{--- (7)}$$

where N corresponds to the number of profiles. The determination of BL height by this method is illustrated in Fig.4. The limitations of VCM are most obvious in the atmosphere, where shear-induced presence of turbulence within the residual layer [27] is responsible for false detections near the ABL.

IV. INTERCOMPARISON BETWEEN METHODS

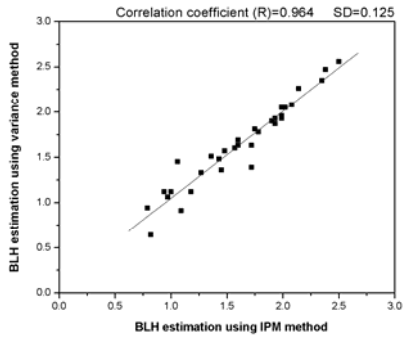


Fig. 5 Correlation plotted between inflexion point and variance methods in estimation of BL height from lidar data. The comparison of correlation was carried out for the lidar data collected between 3 January 2005 and 31 March 2005 taken at mid-night hours

Lidar signals, $S(z)$, measured within 5 min integration are sufficient to determine the ABL height with the GM, LGM and IPM methods. However, the variance method requires averaging of signal profiles over 5 to 60 minutes time frame. It was observed that both the GM and LGM retrieve higher MLD than compared to the IPM method. This is normal since the inflexion point of the first derivative appears just below the GM derivative minimum. A good agreement was found among the different BL determination methods with correlation coefficient larger than 0.96. Fig.5 shows an excellent agreement between IPM and variance lidar analysis methods for the lidar data collected between 3 January 2005 and 31 March 2005. The correlation comparison was carried out for the lidar data taken at midnight hours during cloud free nights of 2005 winter period.

The results of application of GM, IPM and variance methods to Diurnal variation of lidar data, $S(z)$, are shown in Fig.6. The study was carried out on lidar data collected on 7 February 2005. Computational results from different methods show that there is a fine agreement observed between gradient and IPM methods, where as the outcome of variance method with 5 min variability differs from other methods during RL presence. However, it was observed that after execution of higher time integration, the variance method meets the result of other methods.

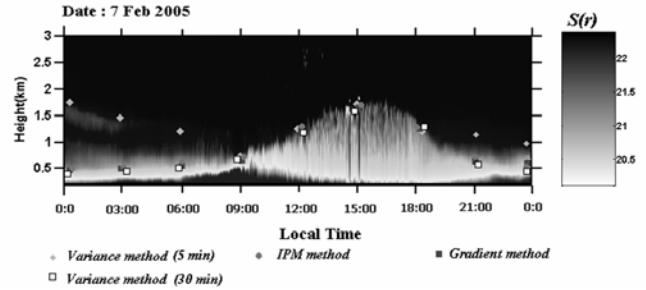


Fig.6 ABL top heights determined using the gradient, IPM, and variance methods shown at 3 hour interval for clarity sake. The lidar data shown was a diurnal data collected on 7 February 2005 at Gadanki site.

Near simultaneous MLD comparisons were carried out at Gadanki site in year 2007 and 2008 using the BLL system and the regular GPS radiosonde soundings. The GPS radiosoundings performed at 12:00 GMT time on regular basis at Gadanki site have been used for the comparison study. Relative humidity values from GPS radiosondes correlate very well with the layers detected by the lidar. Humidity effects can be important on the lidar data through a swelling of the aerosols and an increase of its effective cross section. MLD estimated from lidar using different analytical methods agrees reasonably well with those expected from radiosonde temperature and relative humidity profiles. The outcome of the mixer layer depth (MLD) comparisons between lidar (IPM and variance methods) and radiosoundings are shown in Fig.7 for a part of the study period conducted in January 2008.

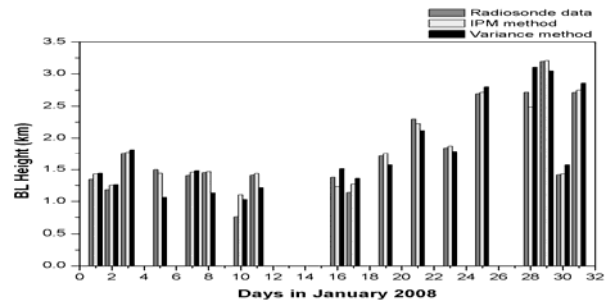


Fig.7 Comparison of lidar methods of MLD estimation (IPM and VCM) and the MLD retrieved from radiosoundings. The study was carried out using the near coincident lidar and GPS radiosonde data obtained during the measurement period January 2008

ACKNOWLEDGMENT

One of the authors, Y.Bhavani Kumar, would like to thank NARL and Atmospheric Science Programme (ASP) Office of ISRO for funding the project BLL and necessary support extended to operate the BLL system during the project period.

REFERENCES

1. Stull, R. B., An introduction to boundary layer meteorology, Kluwer Academic Publishers, Netherlands, 1988.
2. Seibert P., P H. Kromp-Kolb, A. Kasper, M. Kalina, H.Puxbaum, D. T. Jost, M. Schwikowski, and U.Baltensperger, Transport of polluted boundary layer air from the Fohn Valley to high-alpine sites. Atmos. Environ., 32, 3953-3965, 1998.
3. Seibert P., F. Beyrich, S. E. Gryning, S. Joffre, A. Rasmussen, and P. Tercier, Review and intercomparison of operational methods for

- the determination of the mixing height. *Atmos. Environ.*, 34, 1001-1027, 2000.
4. Kunkel, K.E., E.W.Eloranta, and J.A.Weinman, Remote Determination of Winds, Turbulence Spectra, and Energy Dissipation Rates in the Boundary Layer from Lidar Measurements, *J.Atmos.Sci.*, 37, 978-985, 1980.
 5. Boers, R., A parameterization of the depth of the entrainment zone, *J. Appl. Meteor.*, 28, 107-111, 1988.
 6. Boers R., E.W. Eloranta, and R.L.Coulter, Lidar observations of mixed layer dynamics: Tests of parameterized entrainment models of mixed layer growth rate, *J.Climate Appl. Meteor.*, 23, 247-266, 1984.
 7. Crum, T.D., R.Stull, and E.W.Eloranta, Coincident Lidar and Aircraft Observations of Entrainment into Thermals and Mixed Layers, *J.Climate and Appl.Meteorol.*, 26, 774-788, 1987.
 8. Boers, R. and E. W. Eloranta, Lidar measurements of the atmospheric entrainment zone and potential temperature jump across the top of the mixed layer, *Boundary -Layer Meteorol.*, 34, 357-375, 1986.
 9. Cooper, D.I., W.E. Eichinger, M.V.Hynes, D.F.Keller, C.F. Lebeda, and D.A.Poling, High Resolution Properties of the Equatorial Pacific Marine Atmospheric Boundary Layer from Lidar and Radiosonde Observations, *J.Atmos.Sci.*, 53, 2054-2075, 1996.
 10. Bhavani Kumar, Y., "Portable lidar system for atmospheric boundary layer measurements," *Opt. Eng.* Vol 45, 7, 076201, 2006.
 11. Measures, R., *Laser remote sensing*, John Wiley & Sons, Inc., USA, 1984.
 12. Fernald, F., Analysis of atmospheric lidar observations: some comments, *App.Opt.*, 23, 652-653, 1984.
 13. Klett, J. D., Lidar inversion with variable backscatter/extinction ratios, *App.Opt.*, 24, 1683, 1985.
 14. Sasano, Y., and H.Shimizu, N.Sugimoto, I.matsui, N.Takeuchi, and M.Okuda, Diurnal Variation of the Atmospheric Boundary Layer Observed by a Computer Controlled Laser Radar, *J.Meteor. Soc.Of Japan*, 58, 143-148, 1980.
 15. Melfi S.H, J.D. Spinhirne, S.H. Chou and S.P. Palm, Lidar observations of vertically organized convection in the Planetary Boundary Layer over the ocean, *J. Climate Appl. Meteorol.*, 24, 806-821, 1985.
 16. Dupont, E., J.Pelon, And C.Flamant, Study of the Moist Convective Boundary-layer by Backscattering Lidar, *Boundary Layer Meteorol.*, 60, 1-25, 1994.
 17. Kovalev, V.A., and W.E. Eichinger, *Elastic Lidar - Theory, Practice, and Analysis Methods*, Wiley Interscience, 615 pages, 2004.
 18. Endlich R., E. Ludwig and E. Uthe, An automatic method for determining the mixed depth from lidar observations, *Atmos. Environ.*, 13, 1051-1056, 1979.
 19. Flamant C., J.Pelon, P.H.Flamant, and P.Durand, Lidar determination of the entrainment zone thickness at the top of the unstable marine atmospheric boundary layer, *Boundary.-Layer Meteorol.*, 83, 247-284, 1997.
 20. Kaimal, J., N. Abshire, R. Chadwick, M. Decker, W. Hooke, R. Kropfli, W. Neff, F. Pasqualucci, and P. Hildebrand, Estimating the depth of the daytime Convective Boundary Layer, *J.Appl.Meteorol.*, 21, 1123-1129, 1982.
 21. Hayden, K. L., Anlauf, K. G., Hoff, R. M., Strapp, J. W., Bottenheim, J. W., Wiebe, H. A., Froude, F. A., Martin, J. B., Steyn, D. G., and McKendry, I. G., The Vertical Chemical and Meteorological Structure of the Boundary Layer in the Lower Fraser Valley during Pacific 93, *J.Atmos. Environ.* 31, 2089-2105, 1997.
 22. Menut, L., Flamant, C., Pelon, J., and Flamant, P. H., Urban boundary-layer height determination from lidar measurements over the Paris area, *Appl. Opt.* 38, 945-954, 1999.
 23. White, A. B., C. J. Senff, and R. M. Banta, A comparison of mixing depths observed by ground-based wind profilers and airborne Lidar, *J. Atmos.Oce, Tech.*, 16, 584-590, 1999.
 24. Sicard, M., C. Pérez, F. Rocadenbosch, J. M. Baldasano, D. García-Vizcaino, Mixed-Layer Depth Determination in the Barcelona Coastal Area From Regular Lidar Measurements: Methods, Results and Limitations. - *Bound.-Layer Meteor.* 119, 135-157, 2006.
 25. Hooper, W. P., and Eloranta, E. W., Lidar measurements of wind in the planetary boundary layer: the method, accuracy and results from joint measurements with radiosonde and Kyttoon, *J. Climate Appl. Meteorol.* 25, 990-1001, 1986.
 26. Piironen, A., and E.W.Eloranta, Convective Boundary Layer Mean Depths, Cloud Base Altitudes, Cloud Top Altitudes, Cloud Coverages, and Cloud Shadows Obtained from Volume imaging Lidar data, *J. Geoph.Res.*, 100, 25569-25576m, 1995.
 27. Cooper, D. I., W. E. Eichinger, D. Hof, D. Jones, C. R. Quick, and J. J. Tiee, Observations of coherent structures from a scanning lidar, *Agri. and Forest Meteorol.*, 67, 137-150, 1994.

AUTHORS PROFILE



Dr. Y. Bhavani Kumar currently working as Project Leader for LIDAR project at NARL. He has realized several lidar systems such as portable micropulse lidar, Resonance Lidar, Dual polarization Lidar, Infrared backscatter lidar and recently Raman lidar for studies related to the atmosphere.



Mr. S. Purusotham is currently working as a research scholar in the Department of Mathematics, Sri Venkateswara University, Tirupati.